Pressure dependence of the elastic moduli in aluminum-rich Al-Li compounds

Michael J. Mehl*
Complex Systems Theory Branch, Naval Research Laboratory, Washington, D.C. 20375-5320
and Institut Romand de Recherche Numérique en Physique Matériaux, PHB-Ecublens, 1015 Lausanne, Switzerland
(Received 13 July 1992)

I have carried out numerical first-principles calculations of the pressure dependence of the elastic moduli for several ordered structures in the aluminum-lithium system, specifically fcc Al, fcc and bcc Li, $L1_2$ Al_3Li, and an ordered fcc Al_7Li supercell. The calculations were performed using the full-potential linear augmented plane-wave method (LAPW) to calculate the total energy as a function of strain, after which the data were fit to a polynomial function of the strain to determine the modulus. A procedure for estimating the errors in this process is also given. The predicted equilibrium lattice parameters are slightly smaller than found experimentally, consistent with other local-density-approximation (LDA) calculations. The computed elastic moduli are within approximately 10% of the experimentally measured moduli, provided the calculations are carried out at the experimental lattice constant. The LDA equilibrium shear modulus $C_{11} - C_{12}$ increases from 59.3 GPa in Al, to 76.0 GPa in Al_7Li, to 106.2 GPa in Al_3Li. The modulus C_{44} increases from 38.4 GPa in Al to 46.1 GPa in Al_7Li, then falls to 40.7 GPa in Al_3Li. All of the calculated elastic moduli increase with pressure with the exception of bcc Li, which becomes elastically unstable at about 2 GPa, where $C_{11} - C_{12}$ vanishes.

I. INTRODUCTION

The ductility, light weight, and high strength of aluminum make it the best choice for many areas of construction. It can, however, be improved. The addition of small amounts of lithium will greatly increase the strength of the alloy with little change in the ductility.[1] In particular, Young's modulus increases from 70 GPa in pure aluminum to 94 GPa when the atomic concentration of lithium reaches 32%.[2] The experimental value of $C_{11} - C_{12}$ in the metastable $L1_2$ phase of Al_3Li is some 50% larger than it is in pure Al.[3]

In order to study the effect of lithium additions on aluminum, I used the linear augmented plane-wave (LAPW) method[4] to calculate the equation of state and the pressure dependence of the elastic moduli of fcc aluminum, fcc and bcc lithium, the $L1_2$ phase of Al_3Li, and an ordered fcc Al_7Li superlattice. The results of these calculations may be used as a database for fitting approximate methods, such as the Connolly and Williams (CW) method,[5] the generalized Ising Hamiltonian method,[6] or the embedded atom method.[7] Although calculations of this type have been carried out in the Al-Li system to determine the phase diagram,[8,9] the elastic moduli were not computed at that time.

The results of these calculations are interesting in their own right because they show the behavior of Al_xLi over a wide range of pressures. They also demonstrate the accuracy which can be achieved by the LAPW method even when the difference in energies between the different structures is very small (less than 1 mRy).

The outline of this paper is as follows. In Sec. II I summarize the methods used for calculating elastic moduli. Section III shows how to estimate the errors in the calculations. The results (C_{ij} versus pressure) are presented in Sec. IV. Section V contains a summary of the results.

II. CALCULATION OF THE ELASTIC MODULI

A previous paper[10] described the method used to determine the elastic moduli of intermetallic alloys from total energy calculations. I will present a brief review of the method here.

The total energy calculations are carried out using a full-potential version[11] of the linear augmented plane wave method[4] (the LAPW method). The transformation from the many-body problem to a single-particle picture is obtained via the Hedin-Lundqvist parametrization[12] of the local density approximation[13] (LDA) to the density functional theory.[14] The LAPW method treats the core states (here the Al $1s$, $2s$, and $2p$ states, as well as the Li $1s$ states) fully relativistically, and treats the conduction bands in the semi-relativistic approximation.[15] The lattice is divided into muffin-tin spheres and an interstitial region. Inside the muffin tins the basis functions are expanded into spherical harmonics up to order $l = 8$. In the interstitial region the basis functions are expanded into plane waves. I experimented with the basis set cutoff, and found that at the equilibrium volume approximately 40 wave functions/atom were sufficient in the sense that the predicted elastic moduli did not change when I increased the number of basis functions. The single-particle potential is also expanded into spherical harmonics and plane waves, however, the spherical harmonic expansion inside the muffin tins is only carried out up to terms of order $l = 4$. The Brillouin-zone integrations were performed using the Monkhorst and Pack special **k**-point prescription,[16] with modifications to properly treat the special **k**-points in reduced symmetry lattices.[10]

The elastic moduli of a cubic crystal may be divided into two classes, the bulk modulus $B = (C_{11} + 2C_{12})/3$, and the two shear moduli, $C_{11} - C_{12}$ and C_{44}. The bulk modulus is related to the curvature of $E(V)$,

$$B(V) = -VP'(V) = VE''(V) , \quad (1)$$

where V is the volume of the unit cell, $E(V)$ is the energy/unit cell at volume V, and $P(V) = -E'(V)$ is the pressure required to keep the cell at volume V. Since the calculations only provide a set of energies $E(V_i)$ for a limited number of volumes V_i, the second derivative $E''(V)$ must be approximated. Here I begin by making a least squares fit of the computed energies to the form proposed by Birch:[17]

$$\begin{aligned} E(V) = E_o &+ \tfrac{9}{8}B_oV_o[(V_o/V)^{2/3} - 1]^2 \\ &+ \tfrac{9}{16}B_o(B_o' - 4)V_o[(V_o/V)^{2/3} - 1]^3 \\ &+ \sum_{n=4}^{N} \gamma_n[(V_o/V)^{2/3} - 1]^n , \end{aligned} \quad (2)$$

where E_o, V_o, B_o, and B_o' are, respectively, the equilibrium energy, volume, bulk modulus, and pressure derivative of the bulk modulus, while N is the order of the fit. For a second-order fit ($N = 2$) it is obvious that $B_o' = 4$. Experimentally, B_o' is usually between 3 and 5. The bulk modulus can then be obtained by analytic differentiation of (2).

The shear moduli require knowledge of the derivative of the energy as a function of a lattice strain.[18] In the case of a cubic lattice, it is possible to choose this strain so that the volume of the unit cell is preserved. The strain can also be chosen so that the energy is an even function of the strain, whence an expansion of the energy in powers of the strain contains no odd powers. Thus for the calculation of the modulus $C_{11} - C_{12}$ I used the volume-conserving orthorhombic strain tensor,

$$\overleftrightarrow{\varepsilon} = \begin{pmatrix} \delta & 0 & 0 \\ 0 & -\delta & 0 \\ 0 & 0 & \delta^2/(1-\delta^2) \end{pmatrix} . \quad (3)$$

Application of this strain changes the total energy from its unstrained value to

$$E(\delta) = E(-\delta) = E(0) + (C_{11} - C_{12})V\delta^2 + O[\delta^4] , \quad (4)$$

where V is the volume of the unit cell and $E(0)$ is the energy of the unstrained lattice at volume V. For the elastic modulus C_{44}, I used the volume-conserving monoclinic strain tensor

$$\overleftrightarrow{\varepsilon} = \begin{pmatrix} 0 & \frac{1}{2}\delta & 0 \\ \frac{1}{2}\delta & 0 & 0 \\ 0 & 0 & \delta^2/(4-\delta^2) \end{pmatrix} , \quad (5)$$

which changes the total energy to

$$E(\delta) = E(-\delta) = E(0) + \tfrac{1}{2}C_{44}V\delta^2 + O[\delta^4] . \quad (6)$$

Note that there is no pressure or stress term[19] in either (4) or (6) since the strains (3) and (5) are constructed so that $\Delta V = 0$.

The strains (3) and (5) can be used for any cubic lattice. In the general case, the internal parameters of the lattice must be chosen to minimize the total energy of the strained structure. Fortunately, the lattices discussed here fall into a restricted subset of the cubic lattices, where all of the atoms sit at inversion sites, even under the reduced symmetry caused by the strains (3) and (5). For lattices in this class, the atoms will remain on the inversion sites for infinitesimal strains δ. The sites may become unstable at some finite strain, but even then the force on the atoms at the inversion sites will be zero. Since the elastic modulus is only concerned with the limit $\delta \to 0$, it is unnecessary to relax the internal parameters in the strained lattice. This enormously simplifies the calculation.

The use of the strains (3) and (5) reduces the symmetry of the problem compared to the tetragonal and trigonal distortions which are sometimes used.[10] The lower symmetry means that more **k**-points are generated, however, this is compensated by the fact that (4) and (6) are even functions of the strain δ, and so we need only one-half as many calculations. Furthermore, the elimination of the odd powers of δ ensures that $\delta = 0$ will be an extremal point, as required by symmetry.

Having outlined the methods used to calculate the C_{ij}, it must be noted that many compounds, including some of those in the Al-Li system, cannot be grown in single-crystal form, hence the individual elastic moduli cannot be measured experimentally. In these cases experiments can only determine the isotropic bulk B and shear G moduli of polycrystalline aggregates of small crystallites. In the case of the cubic systems discussed here the calculated C_{ij} can be used to determine B exactly and to place rather strict bounds on G. General bounds on B and G were originally determined by Reuss[20] and Voight.[21] Later, Hashin and Shtrikman found improved bounds specific to cubic materials.[22] We will use the later bounds here. For isotropic polycrystalline aggregates of cubic crystallites, the bulk modulus is given exactly by

$$B = \tfrac{1}{3}(C_{11} + 2C_{12}) , \quad (7)$$

just as for a cubic crystal.[23] In true isotropic materials, the shear modulus is related to the elastic moduli by

$$G^I = C_{44}^I = (C_{11}^I - C_{12}^I)/2 , \quad (8)$$

but in real crystals the anisotropy constant

$$A = \frac{2C_{44}}{C_{11} - C_{12}} \quad (9)$$

is not unity. In this case, we can only bound the shear modulus of the aggregate. Hashin and Shtrikman[22] found that for cubic crystals these bounds are given by

$$G_1 = G_1^* + \frac{3(G_2^* - G_1^*)}{5 - 4\beta_1(G_2^* - G_1^*)} \quad (10)$$

and

$$G_2 = G_2^* + \frac{2(G_1^* - G_2^*)}{5 - 6\beta_2(G_1^* - G_2^*)} , \quad (11)$$

where

$$G_1^* = \tfrac{1}{2}(C_{11} - C_{12}), \quad G_2^* = C_{44} \quad (12)$$

and

$$\beta_1 = -\frac{3(B+2G_1^*)}{5G_1^*(3B+4G_1^*)}, \quad \beta_2 = -\frac{3(B+2G_2^*)}{5G_2^*(3B+4G_2^*)} . \tag{13}$$

The Shtrikman bound G_S is designated as the smaller of G_1 and G_2, while the Hashin bound G_H is the larger. Note that in the limit of an isotropic lattice ($A = 1$, or $G_1^* = G_2^*$) we get $G_S = G_H = G$.

In the Al-Li system these bounds are so tight that the difference $|G_H - G_S|$ is on the order of the uncertainty in the calculation of the individual C_{ij}. Thus I will use

$$G = \tfrac{1}{2}(G_S + G_H) \tag{14}$$

as the definition of the shear modulus. The estimated error in G is on the order of the estimated error in the individual C_{ij}. Associated with the bulk and shear modulus are Young's modulus

$$E = \frac{9BG}{3B+G} \tag{15}$$

and Poisson's ratio

$$\sigma = \frac{1}{2}\left(1 - \frac{E}{3B}\right) \tag{16}$$

for isotropic crystals. Since these quantities are often of interest I will list them in the results.

III. ESTIMATING ERRORS

Using Eqs. (4) and (6), the elastic moduli $C_{11} - C_{12}$ and C_{44} are simply related to the second derivative of $E(\delta)$ at zero strain. If δ' is an infinitesimal strain, then, since we have eliminated terms linear in δ,

$$\alpha = \lim_{\delta' \to 0} \frac{E(\delta') - E(0)}{V\delta'^2} , \tag{17}$$

where α is the linear combination of the C_{ij} associated with the strain δ. In principle, we could pick a small, finite strain δ, calculate $E(\delta)$ and $E(0)$, and use (17) to estimate the elastic modulus. In practice, however, numerical errors, which cause fluctuations in the computed $E(\delta)$, make the calculated value of α change rapidly and unpredictably with δ unless great care is taken to ensure convergence in both **k**-points and basis set size.

To avoid this difficulty, it is better to choose a set of M points δ_i and fit the resulting $E(\delta)$ to a polynomial of the form

$$\epsilon_N[\{f_n\};\delta] = \sum_{n=0}^{N} f_n \delta^{2n} . \tag{18}$$

The polynomial (18) contains no odd powers in δ because these terms have been eliminated from the expansions (4) and (6). The quantity f_1/V plays the role of α in Eq. (17). Note that f_1 may still be very sensitive to the choice of N and the δ_i. We need a reliable procedure for determining the best value of f_1 from the available data. This procedure should determine the order $2N$ of the polynomial expansion (18), and also give some estimate of the possible values of f_1 which would give a nearly equivalent fit. To do this analysis, I have chosen to follow a method outlined in the *Numerical Recipes* book.[24]

The calculation of an elastic modulus C_{ij} from total energy calculations begins by choosing a set of M points δ_i, $\{i = 1, 2, ..., M\}$. Typically I choose $M = 5$, with $\delta_1 = 0$ and $\delta_5 \approx 0.05$. If the δ_i are equally spaced, then for the aluminum-bearing compounds discussed here $\Delta E_i = E(\delta_{i+1}) - E(\delta_i)$ is on the order of 1 mRy. Smaller values of ΔE may cause excess numerical noise to introduce large uncertainties in the analysis.

To fit (18) there must be an energy E_i and an error estimate σ_i for each δ_i. I estimated E_i and σ_i by performing LAPW total energy calculations on several **k**-point meshes. For fcc Li and Al I used meshes corresponding to 32 000, 42 592, and 55 296 points in the full Brillouin zone. Symmetry reduced the actual number of points to no more than 7200 in the irreducible part of the Brillouin zone. For structures with larger unit cells and hence smaller Brillouin zones, correspondingly smaller numbers of **k**-points were used. In retrospect, this large number of **k**-points may be excessive, but $\Delta E(\delta)$ in Li is rather small (the energy change between $\delta = 0$ and $\delta = 0.1$ is about 1 mRy), so high accuracy was needed. In any case, since the secular equation was small (about 40 basis functions), these calculations could be done quickly even for large numbers of **k**-points. The energy E_i was calculated by taking an average of the computed $E(\delta_i)$ over the different meshes, weighted by the number of points in the mesh. The uncertainty in the calculation, σ_i, was assumed to be the **k**-point weighted standard deviation about this average. This method of determining σ_i does not include errors associated with other variables in the calculation, including basis set size and the fast Fourier transform mesh size.[25] However, it should give at least an order of magnitude estimate of the size of the error in the calculation.

For a given N, the parameters f_n in (18) are chosen by a least squares fitting procedure, minimizing the quantity

$$\chi^2(N) = \sum_{i=1}^{M} \left(\frac{E_i - \epsilon_N[\{f_n\};\delta_1]}{\sigma_i} \right)^2 . \tag{19}$$

If the numerical errors are normally distributed, the probability that an error less than or equal to $\chi^2(N)$ can occur by chance is

$$q(N) = \int_{\chi^2(N)/2}^{\infty} t^{(M-N-3)/2} e^{-t}\, dt / \Gamma((M-N-1)/2) . \tag{20}$$

For a given compound and lattice constant, the best N is the one which maximizes $q(N)$. Typically, the best q was on the order of 0.5, indicating that our error estimates σ_i were probably too large.[24] (Usual values of σ are on the order of 0.03 mRy for these calculations.) Maximum values of q ranged from 0.05 to 0.95.

As an example of this process, Fig. 1 plots the energy of $L1_2$ Al_3Li as a function of the orthorhombic strain (3) for the fixed volume associated with the cubic lattice constant $a = 7.50$ a.u. ($r_s = 2.93$ a.u.). The $N = 1$ and $N = 2$ fits are also shown. Obviously the $N = 1$ fit ($q = 0.002$) is worse than the $N = 2$ ($q = 0.99$) fit. On

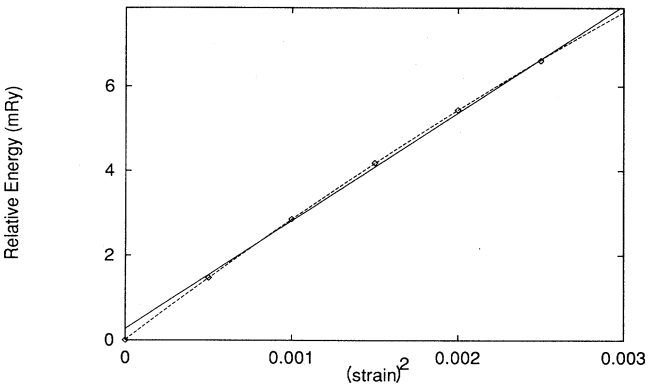

FIG. 1. Energy as a function of the square of the orthorhombic strain (3), used to determine $C_{11} - C_{12}$ in $L1_2$ Al_3Li. The unstrained cubic lattice constant is $a = 7.50$ a.u. ($r_s = 2.93$ a.u.). The error bars, representing the estimated error σ_i, defined in the text, are not shown as they are smaller than the heights of the symbols. The solid line is the $N = 1$ fit (18), the dashed line is the $N = 2$ fit.

the other hand, as seen in Fig. 2, $N = 1$ ($q = 0.68$) and $N = 2$ ($q = 0.74$) fit the monoclinic strain energy (6) equally well.

Once the order N of the fit (18) has been determined, the accuracy of f_1, the parameter related to the elastic modulus, can be established. Assume that the numerical errors in the calculation are normally distributed. Then there is a 68.3% probability that the correct f_1 is within the set of all possible values of f_1 which change $\chi^2(N)$ by less than 2.3. The bounds I present for the elastic moduli are those selected by this formula.

The equilibrium parameters and confidence limits derived from the Birch fit (E_o, V_o, B_o, and B_o') are obtained by similar methods using the functional form (2) and first-principles data $E(V_i)$.

I have written out the above procedure to show how an estimate of the errors in these calculations can be obtained and so that other researchers will be able to obtain the same elastic moduli and estimated uncertainties from the same set of data. The accuracy of these uncertainties is obviously open to question. The errors here are probably not normally distributed. In fact, some systematic errors, such as the change in the energy with respect to basis set size, are not included in the analysis. To conclude, then, these error estimates only serve as a guide to the uncertainty in these calculations.

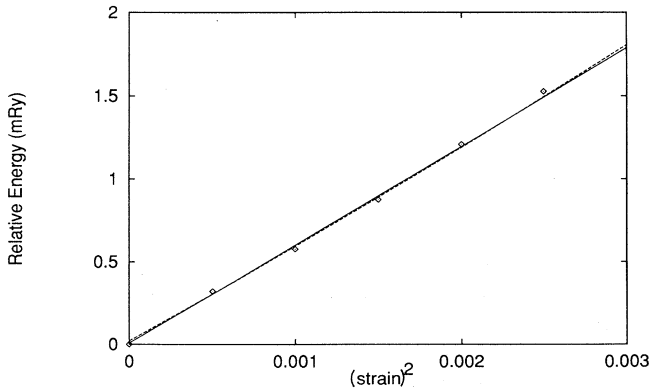

FIG. 2. Energy as a function of the square of the monoclinic strain (5), used to determine C_{44} in $L1_2$ Al_3Li. The unstrained cubic lattice constant is $a = 7.50$ a.u. ($r_s = 2.93$ a.u.). The error bars on the data points, which represent the errors σ_i defined in the text, are omitted as they are almost the same height as the symbols. The solid line is the $N = 1$ fit (18), the dashed line is the $N = 2$ fit.

IV. RESULTS

The results are presented as a series of tables and figures. I first used the LAPW method to calculate the total energy versus volume for fcc Al, fcc Li, $L1_2$ Al_3Li, and ordered Al_7Li in an fcc supercell, as diagrammed in Fig. 3. For completeness, calculations were also performed for bcc Li. The data from these calculations are shown in Fig. 4, where the energy/atom is plotted versus the Wigner-Seitz radius. The data were fit to the Birch equation (2), as described in Sec. III. In all cases the $N = 3$ Birch fits had the best "q" value (20). Table I lists the calculated equilibrium lattice constants, bulk moduli, and pressure derivatives for the $N = 3$ Birch fits. I also list a theoretical binding energy, calculated by finding the difference between the LAPW total/energy atom and the self-consistent total energy of a spherically averaged atom using the Hedin-Lundqvist[12] approximation to the LDA and the semirelativistic approximation[15] for the "valence" orbitals. The computed results are in good agreement with the calculations of Guo and co-

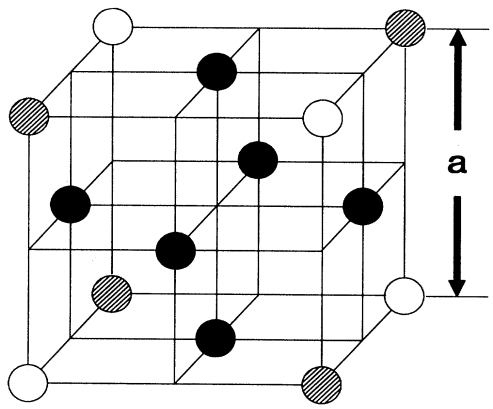

FIG. 3. The fcc based structures used in this paper. The fcc lattice sites are represented by open, shaded, and filled circles. When all sites contain the same type of atom, this represents a simple fcc lattice, with the cube volume equal to four times the volume of the unit cell. If the filled sites are occupied by Al atoms and the open and shaded sites by Li atoms, this represents Al_3Li in the $L1_2$ structure, with the cube shown being the entire unit cell. Finally, if the shaded and filled sites are occupied by Al atoms and the open sites by Li atoms, this represents a part of the fcc supercell Al_7Li lattice. The eight cubes which touch at the lower left-hand corner of the lattice form a cube enclosing four times the volume of the Al_7Li unit cell.

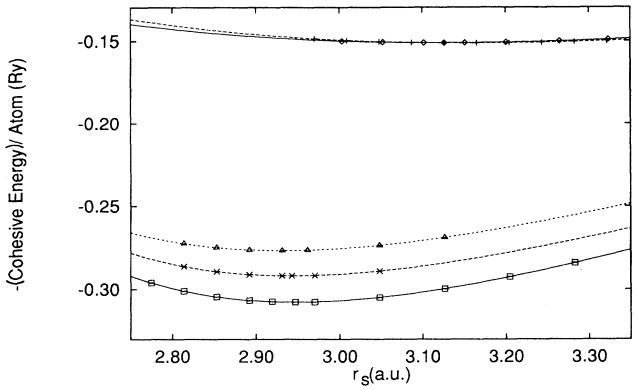

FIG. 4. Computed energy/atom (in rydbergs) versus the Wigner-Seitz atomic radius r_s (in atomic units) for compounds in the Al-Li system. The energy is relative to the atomic energies calculated for spherically averaged atoms. (See the text.) The corresponding $N = 3$ Birch fits (2) are plotted as continuous lines. In the upper part of the graph, the solid line and the "+" represent bcc Li, the dashed line and the "◇" fcc Li. In the lower part of the graph, from the bottom up the curves are fcc Al (solid line and "□"), fcc Al_7Li (dashed line and "×"), and $L1_2$ Al_3Li (dotted line and "△"). The error bars representing the σ_i would be smaller than the size of the markers and so are not shown.

workers,[26,27] which I also present here.

The available experimental data for the lattice constants[28,29] and bulk modulus[30,31] are also listed in Table I. The predicted lattice constants are all smaller than experiment. The error is largest in bcc lithium, where the lattice constant is 3% smaller than experiment.

TABLE I. Equilibrium constants for cubic structures in the Al-Li system, using the $N = 3$ Birch fit (2). The Wigner-Seitz radius r_s is in atomic units, the bulk modulus B_o in GPa, and the cohesive energies E_c in Rydbergs.

	System	r_s	B_o	B_o'	E_c
bcc	Li[a]	3.13	15.1±0.2	3.1±0.5	-0.1511
bcc	Li[b]	3.13	15.0		-0.1245
bcc	Li	3.24[c]	12.0[d]		
fcc	Li[a]	3.16	15.0±0.1	3.4±0.2	-0.1513
fcc	Li[b]	3.12	14.0		-0.1250
fcc	Li	3.24[c]			
fcc	Al[a]	2.95	82.4±0.9	4.8±0.1	-0.308
fcc	Al[e]	2.95	82.0		-0.295
fcc	Al	2.99[c]	76.3[f]		
fcc	Al_7Li[a]	2.94	75.6±0.6	5.0±0.3	-0.292
fcc	Al_7Li[e]	2.94	74.0		-0.283
$L1_2$	Al_3Li[a]	2.93	69.1±0.5	4.7±1.2	-0.277
$L1_2$	Al_3Li[e]	2.94	72.0		-0.272
$L1_2$	Al_3Li	2.95[g]			

[a]Calculated, this work.
[b]Calculated, Ref. 27.
[c]Experiment, Ref. 28.
[d]Experiment, Ref. 30.
[e]Calculated, Ref. 26.
[f]Experiment, Ref. 31.
[g]Experiment, Ref. 29.

The Al and Al_3Li lattice constants are within about 1% of experiment. While some of this is due to the neglect of zero-point motion and thermal expansion, much of the error, especially in lithium, can be attributed to problems with the LDA.[32]

The equation of state, $P(V)$, for these curves can be determined by differentiating the fit (2). The volume dependence of the bulk modulus, $B(V)$, can be found by applying formula (1) to (2). Since $P(V)$ is a monotonic function over the range of volumes shown here it is trivial to numerically invert this function and thus calculate $B(P)$, the pressure dependence of the bulk modulus. Figure 5 plots $B(P)$ for the systems studied in the paper.

The bulk moduli are in reasonably good agreement with experiment. The predicted lithium modulus is about 26% too large, while the Al modulus is 8% too large. The latter error is typical of other calculations.[10] Since the LDA underestimates the equilibrium lattice constant, it is not surprising that it overestimates the bulk modulus. If we use the Birch fit (2) to evaluate the bulk modulus (1) at the experimental lattice constants, we get bulk moduli of 10.6 GPa for bcc lithium and 66.7 GPa for aluminum. These values are both 12% lower than the respective experimental values, overcorrecting the experimental values. It is not clear whether this remaining error is due solely to the LDA or if contributions to the bulk modulus from the thermal and zero-point motion should be included.

The shear moduli were somewhat more difficult to obtain, since the small variation in the total energy as a function of the shear δ required a large **k**-point mesh. The uncertainties in these moduli are usually larger than the uncertainties in B_o. Figures 6 and 7 show $C_{11} - C_{12}$ and C_{44}, respectively, as a function of pressure. The error bars show the estimated uncertainty in the moduli (see Sec. III). The moduli were actually calculated at fixed volume. The pressure was calculated from the Birch fit

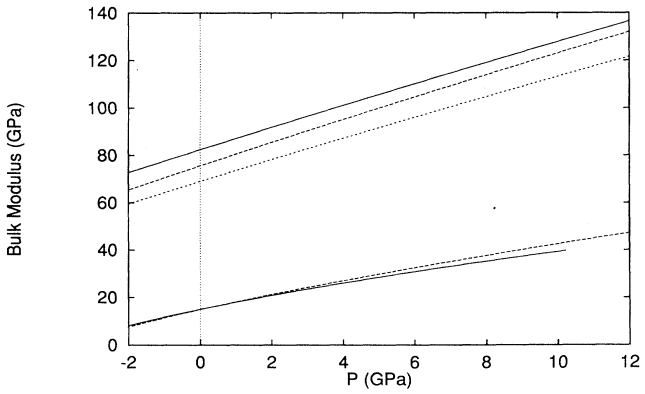

FIG. 5. Computed bulk modulus vs pressure. All units are GPa. Since this is computed from (1), using the Birch fit (2) in Fig. 4, no data points are shown. In the lower part of the graph the solid line represents bcc Li, the dashed line fcc Li. In the upper part of the graph the solid, dashed, and dotted lines represent fcc Al, fcc Al_7Li, and $L1_2$ Al_3Li, respectively. Over this pressure range $B(P)$ can be reasonably approximated by a straight line.

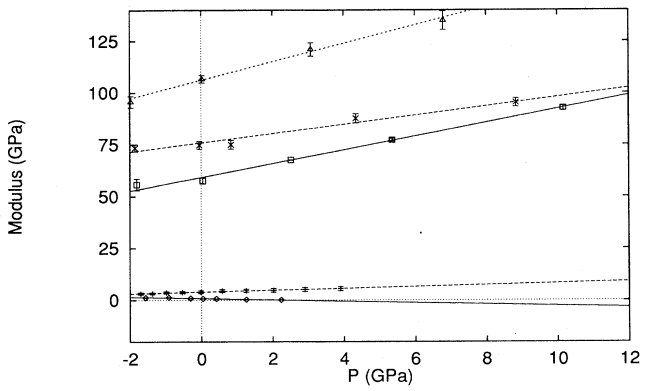

FIG. 6. Shear modulus $C_{11} - C_{12}$ vs pressure. All units are GPa. In the lower part of the graph, the solid line and the "+" represent bcc Li, the dashed line and the "◇" fcc Li. In the upper part of the graph, from the bottom up the curves are fcc Al (solid line and "□"), fcc Al_7Li (dashed line and "×"), and $L1_2$ Al_3Li (dotted line and "△"). The calculation of the error bars is described in Sec. III. The straight lines are least squares fits to the calculated pressure dependence of $C_{11} - C_{12}$, weighted by the estimated error.

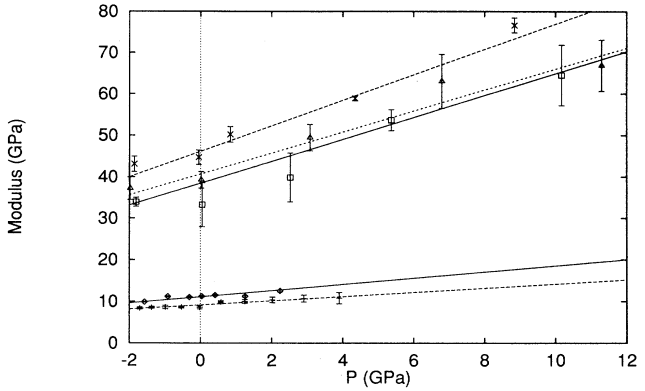

FIG. 7. Shear modulus C_{44} vs pressure. All units are GPa. In the lower part of the graph, the solid line and the "+" represent bcc Li, the dashed line and the "◇" fcc Li. In the upper part of the graph, from the bottom up the curves are fcc Al (solid line and "□"), $L1_2$ Al_3Li (dotted line and "△"), and fcc Al_7Li (dashed line and "×"). The calculation of the error bars is described in Sec. III. The straight lines are least squares fits to the calculated $C_{44}(P)$, weighted by the estimated error. Note that the Al_7Li and Al_3Li curves are reversed compared to Fig. 6.

(2) using $P(V) = -E'(V)$.

As one can see from the figures, the pressure dependence of the elastic moduli can be fit by a straight line, at least over the range −2 GPa to 12 GPa. The lines shown in the figures are determined by a least squares fit to the computed elastic moduli, using the estimated uncertainty as a weighting factor. The intercepts of these lines with the $P = 0$ axis are listed in Table II, while the slopes are in Table III. The estimated errors in the fit are calculated in the manner of Sec. III.

Table II also lists the available experimental data for aluminum,[31] and the Al_3Li calculations of Guo, Podloucky, and Freeman.[33] There is a slight volume discrepancy between the computed aluminum moduli and the experimental numbers, so it is not surprising that the calculated moduli are larger than experiment. Eval-

TABLE II. Equilibrium elastic moduli for cubic structures in the Al-Li system. The Wigner-Seitz radius r_s is in atomic units, and represents the equilibrium lattice constant for computations and the room-temperature lattice constant for experimental measurements. All moduli are in GPa. The last column lists the anisotropy ratio, A (9).

	System	r_s	B	$C_{11} - C_{12}$	C_{11}	C_{12}	C_{44}	A
bcc	Li[a]	3.13	15.1±0.2	0.8±0.1	15.6±0.3	14.8±0.3	11.1±0.2	27.8
fcc	Li[a]	3.16	15.0±0.1	3.9±0.6	17.6±0.5	13.6±0.3	9.1±0.2	4.6
fcc	Al[a]	2.95	82.4±0.9	59.3±1.0	121.9±1.6	62.7±1.3	38.4±3.0	1.3
fcc	Al[b]	2.99	76.3	46.0	107.0	61.0	28.0	1.2
fcc	Al_7Li[a]	2.94	75.6±0.6	76.0±3.0	126.2±2.6	50.3±1.6	46.1±2.7	1.2
$L1_2$	Al_3Li[a]	2.93	69.1±0.5	106.2±3.8	139.8±3.0	33.7±1.7	40.7±2.2	0.8
$L1_2$	Al_3Li[c]		72.3	128.6	158.0	29.4	57.7	0.9

[a]This work.
[b]Experiment, Ref. 31.
[c]Calculations, Ref. 33.

TABLE III. Equilibrium pressure derivatives of the elastic moduli for cubic structures in the Al-Li system. The Wigner-Seitz radius r_s is in atomic units.

	System	r_s	B'	$C'_{11} - C'_{12}$	C'_{11}	C'_{12}	C'_{44}
bcc	Li	3.13	3.1±0.5	-0.3±0.03	2.9±0.6	3.2±0.5	0.7±0.1
fcc	Li	3.16	3.4±0.2	0.4±0.4	3.6±0.5	3.2±0.3	0.5±0.1
fcc	Al	2.99	4.8±0.1	3.3±0.3	7.0±0.4	3.7±0.2	2.6±1.0
fcc	Al_7Li	2.94	5.0±0.3	2.2±0.7	6.5±0.7	4.3±0.5	3.1±0.6
$L1_2$	Al_3Li	2.93	4.7±0.2	4.4±1.2	7.6±0.9	3.2±0.5	2.5±0.7

TABLE IV. Derived properties of aggregate crystals. The moduli B, G_S, G_H, G, and E are in GPa. All calculations are done using the LDA equilibrium moduli in Table II.

	System	B	G_S	G_H	G	E	σ
bcc	Li	15.1	1.6	5.1	3.3	9.3	0.40
fcc	Li	15.0	4.6	5.4	5.0	13.5	0.35
fcc	Al	82.4	34.6	34.6	34.6	91.2	0.32
fcc	Al_7Li	75.6	42.7	42.7	42.7	107.7	0.26
$L1_2$	Al_3Li	69.1	45.3	45.3	45.3	111.5	0.23
$L1_2$	Al_3Li[a]					91.0	

[a]Experiment, Ref. 2, interpolated to 25% lithium content.

uating the moduli at the experimental volume gives $C_{11} - C_{12} = 48.7$ GPa and $C_{44} = 30.1$ GPa, both within 8% of experiment. Combining these numbers with the bulk modulus data shown above, it seems that the LDA can predict the elastic moduli to within about 10%, if the experimental volume is used.

Except for C_{12}, the computed Al_3Li moduli are somewhat smaller than the calculations in Ref. 33 or the experimental results reported there. Those calculated moduli were presumably determined at the experimental volume, so the true discrepancy is somewhat larger than the 42% disagreement in C_{44} shown in the table. However, both sets of calculations agree that there is a large increase in $C_{11} - C_{12}$ with increasing lithium content.

I next used the zero-pressure moduli from Table II to calculate the Hashin-Shtrikman bounds on the shear modulus G for a polycrystalline aggregate. Notice that, except for Li, the bounds on G are smaller than the uncertainties in the original elastic moduli. Thus the actual uncertainties in G are approximately the same as the uncertainties in Table II. Table IV collects the information which can be derived for the aggregate crystals, including the bulk modulus (7), the shear modulus (14), Young's modulus (15), and Poisson's ratio (16). The Young's modulus for several Al-Li compounds has been measured experimentally,[2] and is also presented in Table II. Not surprisingly, the predicted Young's modulus is some 23% larger than the experimental number. Evaluating the modulus at the experimental parameter gives $E = 103$ GPa, within 13% of experiment.

Although not part of the major thrust of this paper, there are several features of interest in the lithium data. Calculations show that fcc Li is 0.2 mRy more stable than bcc Li. Experimentally, bcc lithium may transform to the fcc state at $T = 78$ K,[28] although the actual ground state of lithium is apparently a hexagonal close packed structure. The calculations are also in agreement with earlier works,[34] which agree that the fcc-bcc energy difference is about 0.2 mRy.

The behavior of lithium under pressure is also worthy of note. Figure 6 shows that bcc lithium becomes elastically unstable at about 2 GPa, when the modulus $C_{11} - C_{12}$ vanishes. This is consistent with the ground state of lithium being a close-packed phase.[28] However, the Birch fits to the equation of state show a pressure induced phase transition from fcc lithium *to* bcc lithium near 0.6 GPa. Since the energy difference between the two phases is only 0.2 mRy, it is obvious that thermal and zero-point motion, which are neglected here, must be included to obtain an understanding of the behavior of lithium.

V. SUMMARY

As shown above, addition of lithium into fcc aluminum increases both of the shear moduli. $C_{11} - C_{12}$ is 28% larger in Al_7Li than in pure Al, and 79% larger in Al_3Li than in Al. For C_{44} the increases are 20% and 6%, respectively. Conversely, the bulk modulus decreases slightly with increasing lithium concentration. Since $C_{11} - C_{12}$ and C_{44} increase by nearly the same ratio in going from Al to Al_7Li, the anisotropy factor A (9) is nearly unchanged, while it is much smaller in Al_3Li than it is in either Al or Al_7Li. This increase in anisotropy was also found by Guo, Podloucky, and Freeman,[33] who attributed it to increasing anisotropy of the chemical bonding with the addition of lithium. From the results presented here, it is apparent that the anisotropy ratio does not change appreciably for small amounts of lithium, increasing only when there are large numbers of lithium atoms on next-nearest-neighbor sites (see Fig. 3). However, Poisson's ratio (16) does decrease from 0.32 in Al to 0.26 in Al_7Li, indicating that some anisotropy is present even at this Li concentration. It would be interesting to study the behavior of the anisotropy at smaller lithium concentrations by continuing the elastic moduli calculations for ordered supercells with chemical composition $Al_{15}Li$ or $Al_{26}Li$. Unfortunately, while simple total energy calculations for these structures are possible on present computers, in this case not all of the aluminum atoms are at inversion sites, so relaxation of these atoms around the lithium "impurities" must be included.[35] It would require a large number of total energy calculations to obtain the energies of the relaxed structures needed for the calculation of the C_{ij} in these systems.

The elastic moduli all change linearly with pressure in the region studied (-2 to 12 GPa). There is some variation in the slope of these lines, but generally the slope is between 3 and 5. The exceptions are $C'_{11} - C'_{12}$ and C'_{44} in the lithium structures, which are all less than 1, and C'_{11} in the aluminum compounds, where the slope is about 7.

In conclusion, I have calculated the pressure dependence of the elastic moduli for several ordered Al-Li lattices, including error estimates in the calculation of the elastic moduli. The computations show that the addition of lithium strongly increases the shear moduli and

Young's moduli (by about 20%) over aluminum. The decrease in Poisson's ratio indicates that the lithium introduces anisotropic chemical bonding.

ACKNOWLEDGMENTS

I would like to thank D. A. Papaconstantopoulous, B. M. Klein, and D. Singh for helpful comments and encouragement. Special thanks are due to A. Gonis, who suggested this investigation, and to R. Podloucky, who led me to several references. Parts of this work are supported by the Office of Naval Research, United States Department of Defense.

---

*Current address: Institut Romand de Recherche Numérique en Physique de Matériaux (IRRMA), PHB Ecublens, 1015 Lausanne, Switzerland.

[1]W. Müller, E. Burbeck, and V. Gerald, in *Aluminum-Lithium Alloys III*, edited by C. Baker, P. J. Gregson, S. J. Harris, and C. J. Peel (Institute of Metals, London, 1986).

[2]B. Nobel, J. Harris, and K. Dinsdale, J. Mater. Sci. **17**, 461 (1982).

[3]H. J. Axon and W. Hume-Rothery, Proc. R. Soc. London, Ser. A **193**, 1 (1948); E. D. Levine and E. J. Rapperport, Trans. Metal. Soc. AIME **227**, 1204 (1963).

[4]O. K. Andersen, Phys. Rev. B **12**, 3060 (1975).

[5]B. P. Burton, J. E. Osburn, and A. Pasturel, Phys. Rev. B **45**, 7677 (1992).

[6]S.-H. Wei, L. G. Ferreira, and A. Zunger, Phys. Rev. B **45**, 2533 (1992).

[7]J. A. Rifkin, C. S. Becquart, D. Kim, and P. Clapp (unpublished); C. Becquart, Ph.D. thesis, University of Connecticut, 1992.

[8]M. Sluiter, D. de Fontaine, X. Q. Guo, R. Podloucky, and A. J. Freeman, Phys. Rev. B **42**, 10460 (1990).

[9]R. Podloucky, H. J. F. Jansen, X. Q. Guo, and A. J. Freeman, Phys. Rev. B **37**, 5478 (1988).

[10]M. J. Mehl, J. E. Osburn, D. A. Papaconstantopoulous, and B. M. Klein, Phys. Rev. B **41**, 10311 (1990); **42**, 5362(E) (1991).

[11]S. H. Wei and H. Krakauer, Phys. Rev. Lett. **55**, 1200 (1985).

[12]L. Hedin and B. I. Lundqvist, J. Phys. C **4**, 2064 (1971).

[13]W. Kohn and L. J. Sham, Phys. Rev. **140**, A1133 (1965).

[14]P. Hohenberg and W. Kohn, Phys. Rev. 136, B864 (1964).

[15]D. D. Koelling and B. N. Harmon, J. Phys. C **10**, 2041 (1975).

[16]H. J. Monkhorst and J. D. Pack, Phys. Rev. B **13**, 5188 (1976).

[17]F. Birch, J. Geophys. Res. **83**, 1257 (1978).

[18]C. Kittel, *Introduction to Solid State Physics*, 6th ed. (Wiley, New York, 1986).

[19]M. Alouani, R. C. Albers, and M. Methfessel, Phys. Rev. B **43**, 6500 (1991).

[20]A. Reuss, Z. Agnew. Math. Mech. **9**, 49 (1929).

[21]W. Voight, *Lehrbuch der Kristallphysik* (Tubner, Leipzig, 1928).

[22]Z. Hashin and S. Shtrikman, J. Mech. Phys. Solids **10**, 335 (1962); **10**, 343 (1962).

[23]E. Schreiber, O. L. Anderson, and N. Soga, *Elastic Constants and Their Measurement* (McGraw-Hill, New York, 1973).

[24]W. H. Press, B. P. Flannery, S. A. Teukolsky, and W. T. Vetterling, *Numerical Recipes: The Art of Scientific Computing* (Cambridge University Press, New York, 1986), chap. 14.

[25]S.-H. Wei, Ph.D. thesis, College of William and Mary, Williamsburg, Virginia, 1985.

[26]X.-Q. Guo, R. Podloucky, Jian-hua Xu, and A. J. Freeman, Phys. Rev. B **41**, 12432 (1990).

[27]X.-Q. Guo, R. Podloucky, and A. J. Freeman, Phys. Rev. B **42**, 10912 (1990).

[28]J. Donohue, *The Structures of the Elements* (Wiley, New York, 1974).

[29]W. B. Pearson, *A Handbook of Lattice Spacings and Structures of Metals and Alloys* (Pergamon, Oxford, 1967), Vol. 2.

[30]E. A. Brandes, *Smithells Metals Reference Book*, 6th ed. (Butterworths, Boston, MA, 1983).

[31]G. Simmons and H. Wang, *Single Crystal Elastic Constants and Calculated Aggregate Properties: A Handbook*, 2nd ed. (MIT Press, Cambridge, Massachusetts, 1971).

[32]J. P. Perdew, J. A. Chevary, S. H. Vosko, K. A. Jackson, M. R. Pederson, D. J. Singh, and C. Fiolhais, Phys. Rev. B **46**, 6671 (1992).

[33]X.-Q. Guo, R. Podloucky, and A. J. Freeman, J. Mater. Res. **6**, 324 (1991).

[34]J. A. Nobel, S. B. Trickey, P. Blaha, and K. Schwarz, Phys. Rev. B **45**, 5012 (1992), and references therein.

[35]For examples of possible lattices and relaxations, see, e.g., M. J. Mehl and B. M. Klein, Physica B **172**, 211 (1991).